Elemental Scientific LASERS
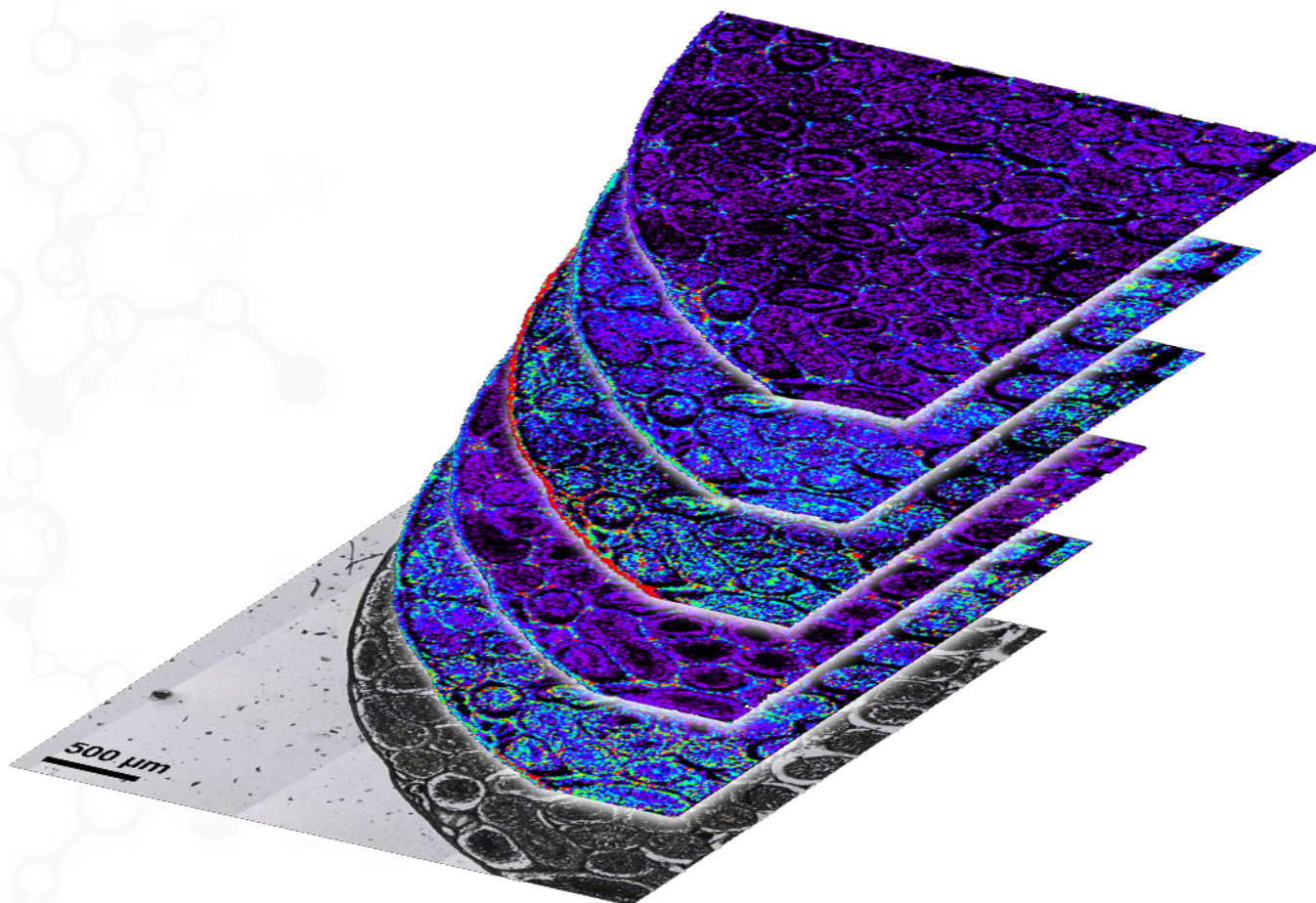
INNOVATION TO ILLUMINATE

Why 266 nm is the ideal wavelength
for bioimaging of biological materials by LA-ICPMS

500 µm

Introduction

The imageBIO266 from Elemental Scientific Lasers (ESL) is the world's first laser ablation system designed from top to bottom solely for bioimaging. Every single component has been created or optimised for this exact application – no half measures and no compromises – from the incredible new TwoVol3 ablation chamber with its sub-millisecond washout speed, to the 20X microscope turret, and the super-stable diode-pumped 266 nm laser.

Here we explain why ESL has made such a bold choice by showing the scientifically proven benefits of using a 266 nm wavelength for bioimaging. Elemental Scientific Lasers collaborated with Professor Barry Sharp and Dr. Amy Managh (University of Loughborough) and Professor Norbert Jakubowski (BAM) over many years to explore different technologies that would enhance laser ablation of biological tissue and firmly concluded that 266 nm is the right choice for bioimaging.
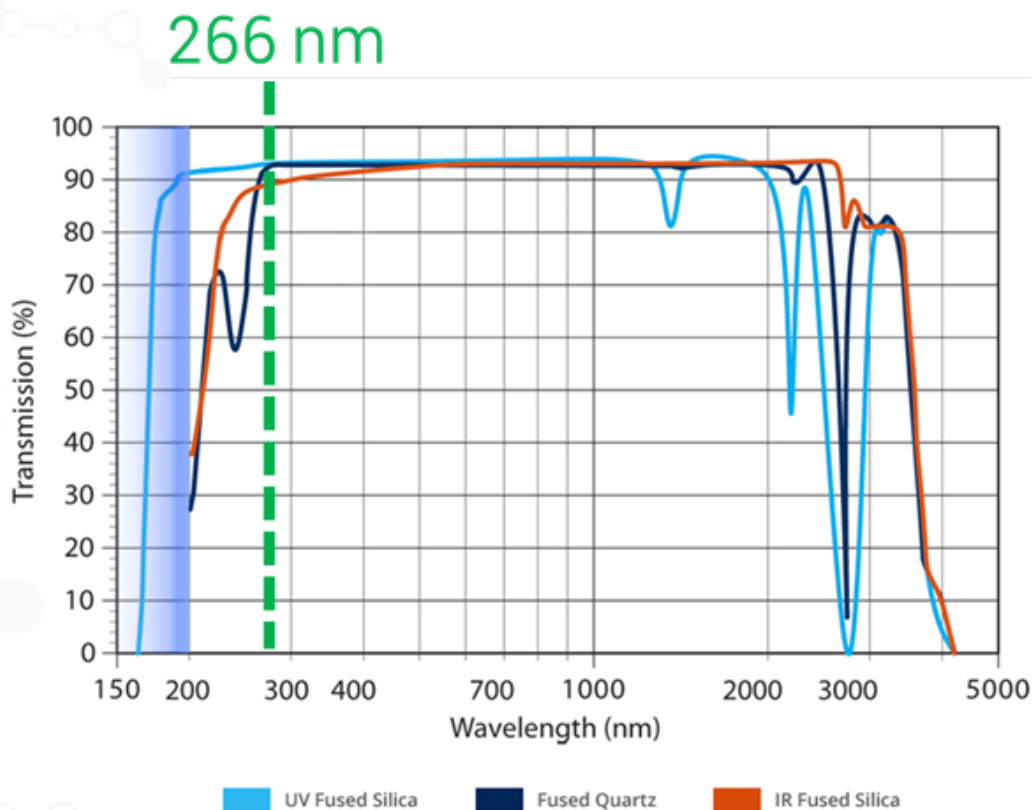
266 nm

Figure 1. Absorption spectrum of quartz and silica. Transmission is highest above 260 nm, indicating that if glass ablation is to be avoided then the laser wavelength should be >266 nm. Coupling with glass is at its maximum below 200 nm.

Tissue Ablation at 266 nm and 193 nm

The majority of biological samples are presented as either cells or microtomed thin sections mounted onto a glass slide. One of the key goals of bioimaging by laser ablation ICPMS is to completely and cleanly remove the entire thickness of sectioned tissue from the glass slide without causing any ablation to the slide. Contributions to the signal from ablated glass are an unknown – essentially a contaminant – and cannot be deconvolved from the total signal after analysis.

Biological tissue couples well with many laser wavelengths so the ideal scenario would be to select a wavelength that is as low as possible but that couples poorly with glass to maximise the band gap between ablation of tissue and ablation of glass. Quartz and silica both absorb strongly below 200 nm, and Figure 1 shows that the transmission reaches its peak at a wavelength of greater than 260 nm. Above this wavelength we can expect excellent ablation of tissue and poor ablation of glass – exactly what is needed to ensure signals from the glass do not contribute to the signal from the tissue. We selected 266 nm as this is the fourth harmonic of a Nd:YAG laser, a robust and reliable laser type, utilized in a wide range of high throughput industries.

At first, this approach may seem counterintuitive. After all we have been schooled into believing that where wavelength is concerned, lower is better. However, this axiom came about because up until now laser ablation development has been driven by the geochemistry market. Geological samples are mostly strongly covalently-bonded crystal structures that require high photon energy for efficient coupling of the laser pulse with the matrix. Biological materials on the other hand are made up of molecules held together by dative bonds that get weaker still when the tissue is dried and sectioned. The tissue is also not chemically bonded at all to the glass substrate underneath.

When we ablate a tissue section on glass with a 193 nm laser the laser pulses couple efficiently with both the tissue and glass substrate underneath (Figure 2), so the energy must be optimized based on the glass and not on the sample itself. The aerosol contains particles from both materials that cannot be separated out in data-processing. We could turn the fluence of the 193 nm laser down, but that leaves us with too little energy to fully ablate the entire thickness of the tissue section. This is because the ablation threshold of the tissue and the glass are both close together, and both below the optimum fluence for ablating tissue.
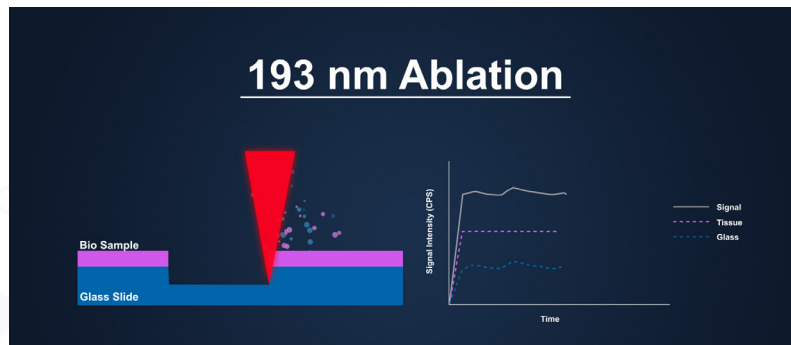

Figure 2. Ablation of biological tissue at 193 nm on a glass substrate can result in ablation of the glass substrate under the tissue, since the deep UV wavelength is optimised for ablation of glassy/mineral phases.
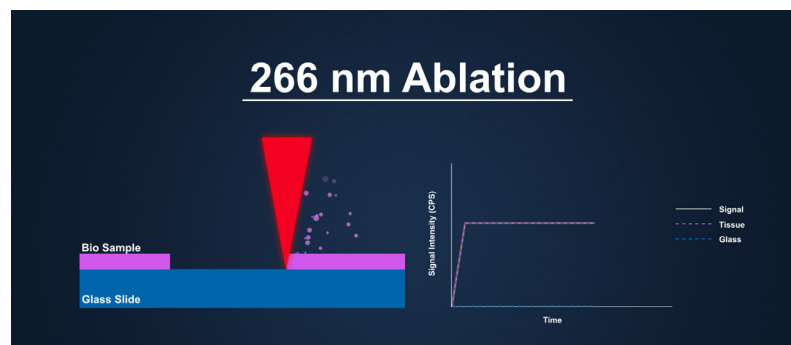

Figure 3. 266 nm couples poorly with glass, leaving a significantly higher bandgap where tissue is ablated and glass is not.

Tissue Ablation at 266 nm and 193 nm
(continued)

By using a 266 nm wavelength we can fully ablate the entire thickness of the tissue before we have reached the ablation threshold of the glass underneath (Figure 3). The poor coupling of the laser with glass means that there is a high bandgap between ablation of tissue and ablation of glass (Figure 4 & Table 1). By choosing this wavelength we can optimise our parameters based on the properties of the sample, and not on the substrate underneath.
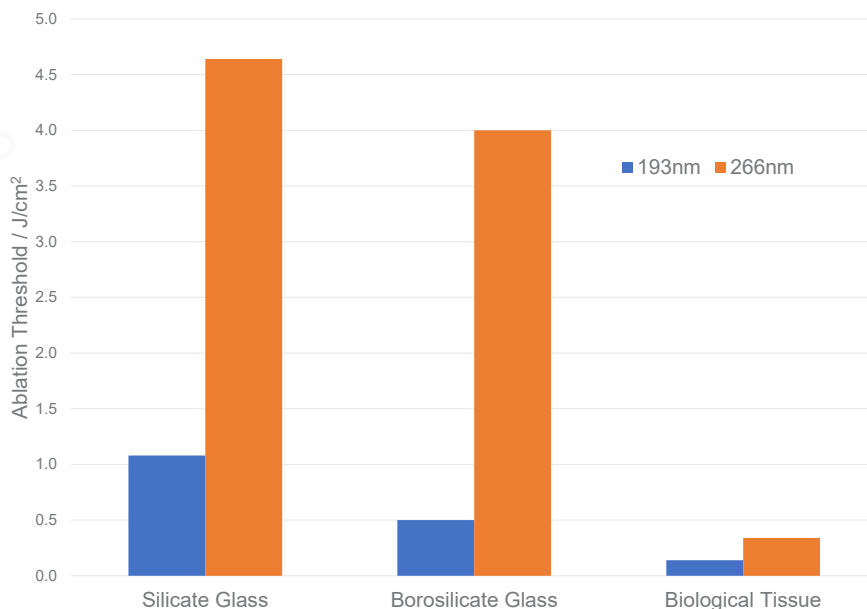

Figure 4. At 193 nm the bandgap between tissue and glass ablation is very small. At 266 nm the bandgap is significantly wider, leading to greater flexibility with operating conditions.

Table 1. Ablation threshold values for different matrices at 193 nm and 266 nm wavelengths.

Matrix	Ablation Threshold @ 193 nm	Bandgap between tissue and glass	Ablation Threshold @ 266 nm	Bandgap between tissue and glass
Silicate Glass	1.08 J/cm² [1]	0.94 J/cm²	4.64 J/cm²	4.30 J/cm²
Borosilicate Glass	0.50 J/cm² [1]	0.36 J/cm²	4.0 J/cm²	3.66 J/cm²
Biological Tissue	0.14 J/cm² [1]	-	0.34 J/cm²	-

The inclusion of borosilicate glass in Table 1 is important. Different glass matrices can have radically different ablation thresholds, and this is not apparent until it has been ablated. At 266 nm this difference relative to the ablation threshold for tissue is miniscule, and therefore, inconsequential. At 193 nm, however, the threshold for borosilicate glass is significantly closer to that of biological tissue than for silicate glass, therefore, there are no such things as "typical method parameters" at this wavelength. Analysts rarely get to make the decision on which type of glass slide is used and usually have to deal with whatever they are given.

The literature all supports this. Van Acker et al.[1] noted that at 193 nm SLS glass and borosilicate glass ablate at fluence levels of just 262 mJ/cm^2 due to the coupling efficiency of the laser at this wavelength, which is close the ablation threshold of tissue and is very close to the minimum output of the laser. Horn et al.[2] demonstrated that 193 nm couples better with glass than 266 nm, and Guillong et al.[3] recommended wavelengths shorter than 213 nm for ablation of silicates.

These milestone publications all suggest that a deep UV wavelength is essential for efficient ablation of glass-like and geological materials, but in bioimaging that is what we must avoid.

Elemental Scientific Lasers have taken the time to perform a real comparison of 266 nm and 193 nm to demonstrate that 266 nm is the right choice for bioimaging. Using a 20 µm square spot we ablated line scans and spot ablations into a tissue standard on quartz glass slides and steadily increased the laser fluence. Each position in the line scan received 5 full pulses of the laser (laser dosing = 5). The fluence at the sample surface of both laser ablation systems was calibrated using a traceable Coherent FieldMaxII energy meter. The tissue standards, provided by Dr. Dominic Hare (Florey Institute, Melbourne, Australia), were produced using spiked, homogenised mouse brain with 10 ppm Cu and Zn, microtomed to a thickness of 5 µm and placed onto a quartz glass microscope slide.

At 193 nm the threshold of ablation for tissue was 0.14 J/cm^2, while the glass begins to ablate at 1.08 J/cm^2 (Figure 5, right). This means that there is a bandgap – where the tissue ablates and the glass does not – of just 0.95 J/cm^2. These values are in agreement with other studies.

When we perform the same experiment using 266 nm we find that the threshold of ablation is 0.34 J/cm^2, while the glass does not ablate below a fluence of 4.64 J/cm^2 (Figure 5, left). The bandgap is significantly higher using 266 nm – 4.30 J/cm^2 – giving a greater range of fluence settings to optimise bioimaging experiments.
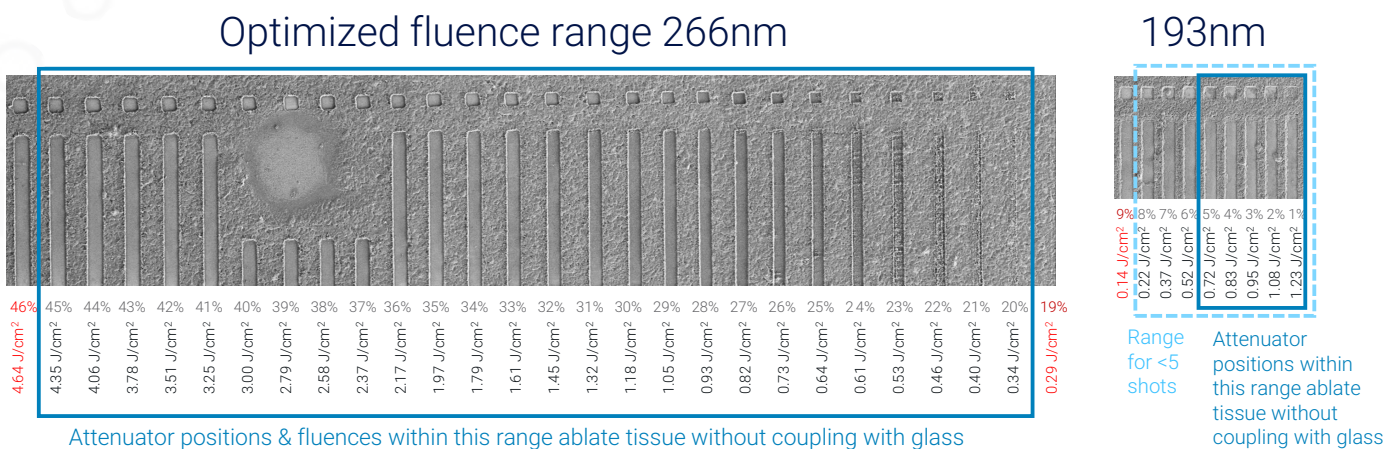

Figure 5. SEM images of ablated tissue in the optimized fluence range for both wavelengths post-ablation. Percentages show the attenuator position of each ablation and blue boxes show the optimized fluence range for each wavelength, where tissue is sampled but glass is not. Experimental parameters were 20x20 µm square spot, 250 µm line, 100 Hz rep rate, 400 µm/s scan speed. Laser dosing is 5 shots per coordinate position.

Tissue Ablation at 266 nm and 193 nm *(continued)*

During these ablations we monitored Cu and Zn, which are doped into this tissue standard, and Al and Si, which we only see when the ablate glass slide underneath the tissue is ablated. The ICPMS data shows that at 193 nm the tissue is not fully consumed until 0.83 J/cm^2 is reached (Figure 6). This reduces our practical bandgap to 0.12 J/cm^2. Compared to a maximum fluence of 15 J/cm^2 for this laser ablation system, the bandgap is < 1% of the full range. The signals for Al and Si steadily increase above 1 J/cm^2, and the orange plot for ^{66}Zn clearly shows an uncontrollable contribution from the glass as fluence increases. Conversely, the ^{63}Cu signal appears to be becoming suppressed as glass particulate joins tissue in the ICP. Furthermore, tissue is only fully ablated in a single shot – required for high speed imaging (e.g. time of flight) – at a fluence of 4 J/cm^2. At 193 nm this is nearly four times the ablation threshold of glass and a contribution to the signal from glass ablation is all but guaranteed.
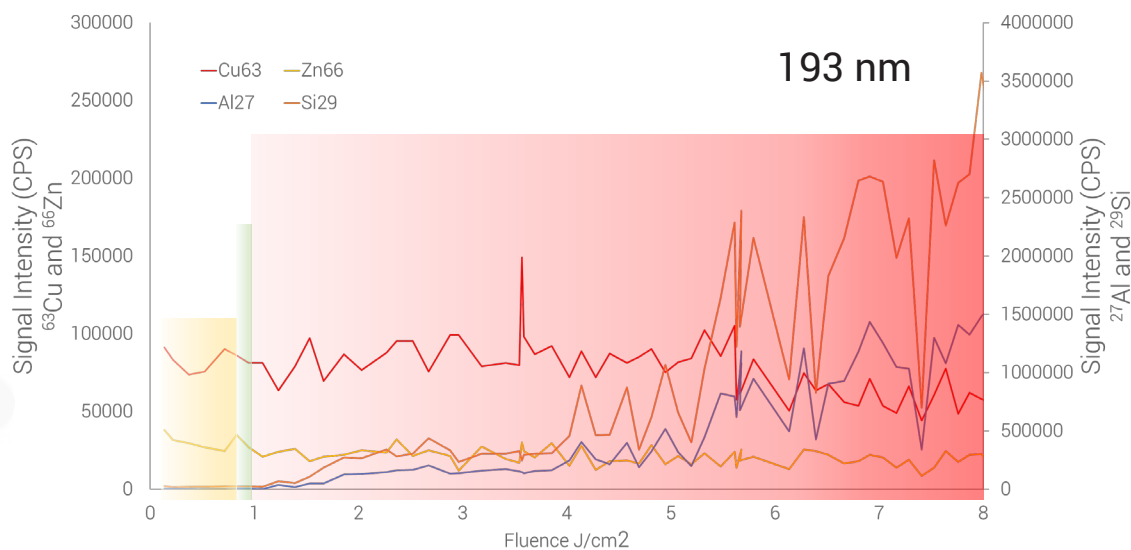

Figure 6. Signals resulting from ablation of tissue on quartz glass using a 193 nm laser. The threshold of ablation for tissue is 0.14 J/cm^2, however, the entire thickness is not fully ablated until 0.83 J/cm^2, and the threshold of ablation for the glass slide is 1.08 J/cm^2. This leaves a working range of 0.83 to 0.95 J/cm^2 – < 1% of the fluence range of the instrument.

At 266 nm the threshold of ablation for tissue is 0.34 J/cm^2, and the tissue is fully consumed in 5 shots at 0.93 J/cm^2. The threshold for glass ablation is 4.64 J/cm^2 giving a working range of 3.71 J/cm^2 (Figure 7). Crucially, the tissue can be fully ablated in a single shot at 3.78 J/cm^2, which is still below the ablation threshold for glass at this wavelength. Signals for ^{63}Cu and ^{66}Zn are stable throughout the fluence range.
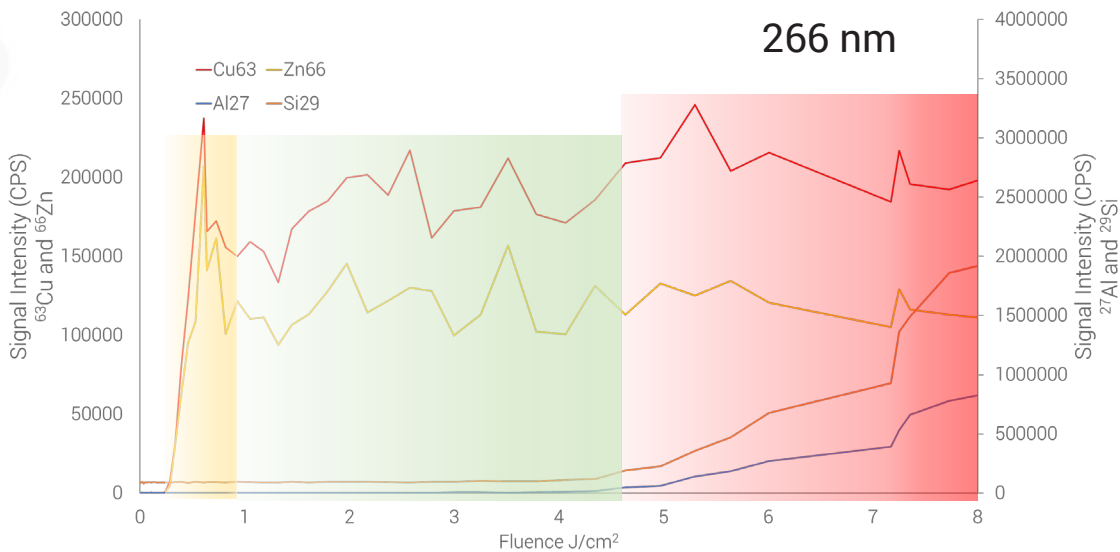

Figure 7. Signals resulting from ablation of tissue on quartz glass using a 266 nm laser. The threshold of ablation for tissue is 0.34 J/cm^2=, and the entire thickness is fully ablated in 5 shots above 0.93 J/cm^2. The threshold of ablation for the glass slide is 4.64 J/cm^2.

If we compare 193 nm with 266 nm we can draw further conclusions. Sensitivity of Cu is similar between both wavelengths below the ablation threshold of the glass, but above this there also appears to be a contribution to the Cu signal from the ablated glass. The signal is significantly more stable as we alter fluence on the 266 nm system. The signal intensity of Zn on the 266 nm system is double that of the 193 nm system. Considering that both lasers are consuming the entire thickness of the sample, the signal intensities and stability should be identical.

Improvements in Laser Robustness and Cost of Ownership

In addition to the analytical, there are huge benefits to using an air-cooled, diode-pumped Nd:YAG 266 nm laser instead of an excimer, water cooled 193 nm. DPSS lasers have proven performance over hundreds of billions of shots in the high throughput semiconductor industry, where they are used for the precise cutting of electronic materials and wafers (Figure 8). An excimer laser system requires ArF gas, which is expensive, has health and safety implications, and requires regular exchange, sometimes during an imaging experiment.

It also requires that the beam path be purged using high grade nitrogen at all times. The Nd:YAG rod and diode array of the 266 nm system do not require any intervention for billions of shots. The output is stable in the short and long term. Excimer systems are large, whereas the imageBIO266 is a benchtop system. Additionally, laser optics at 266 nm are significantly more robust than their deep-UV equivalents and will last much longer.
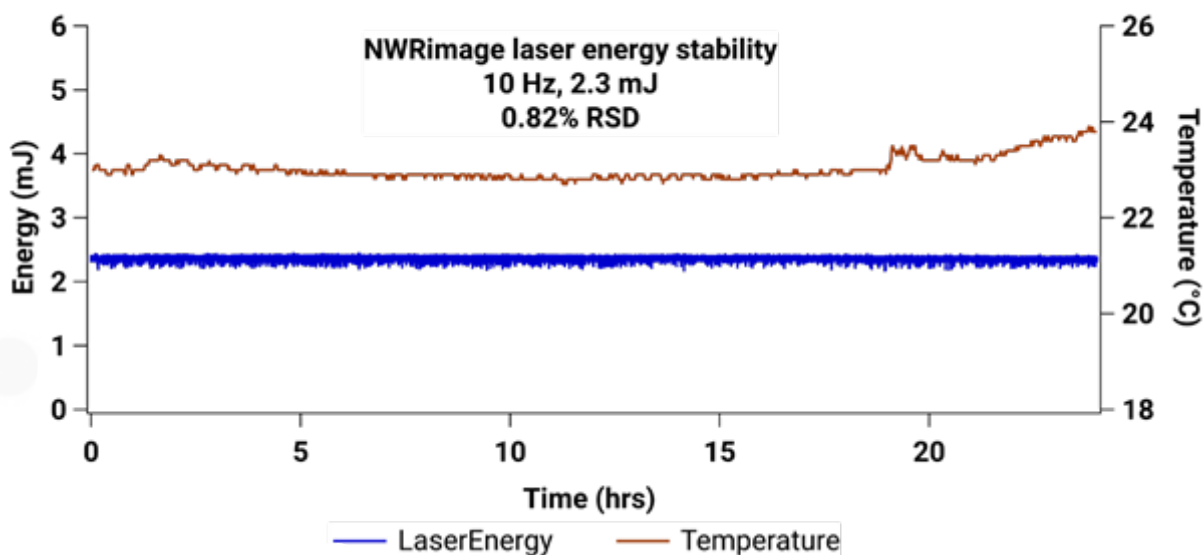
Figure 8. 24 hour stability of the Polaris laser used in the imageBIO266 is 0.82% RSD in an environment with temperature changes. This level of stability is essential for bioimaging experiments that can run into days or even weeks.

imageBIO266 with standard chamber (left) and TwoVol3 ablation chamber (above).
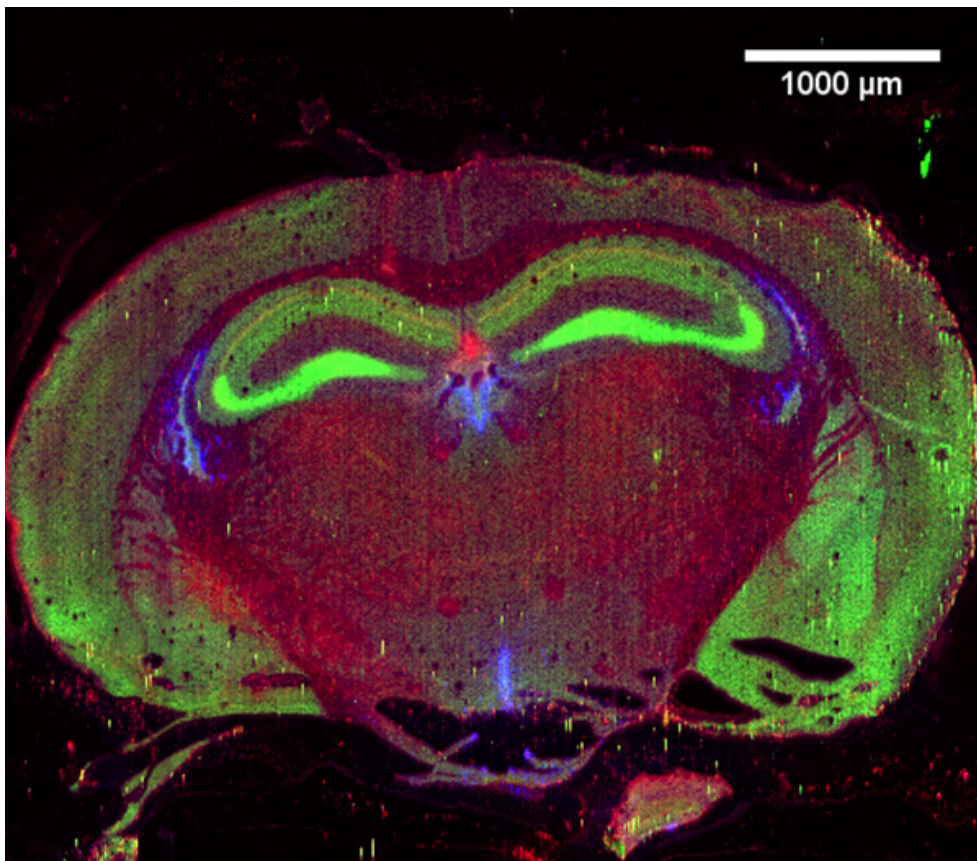
Examples of Bioimaging at 266 nm

Figure 9. A cross sectional image of age related changes of Fe (red), Zn (green) and Cu (blue) in mouse brain using a 10 μm spot, 100 Hz repetition rate. Image area: Area of 5.5 x 4.5 mm. Analysis time of 41 minutes. Samples courtesy of Northwestern University. Analysis at LGC using imageBIO266.
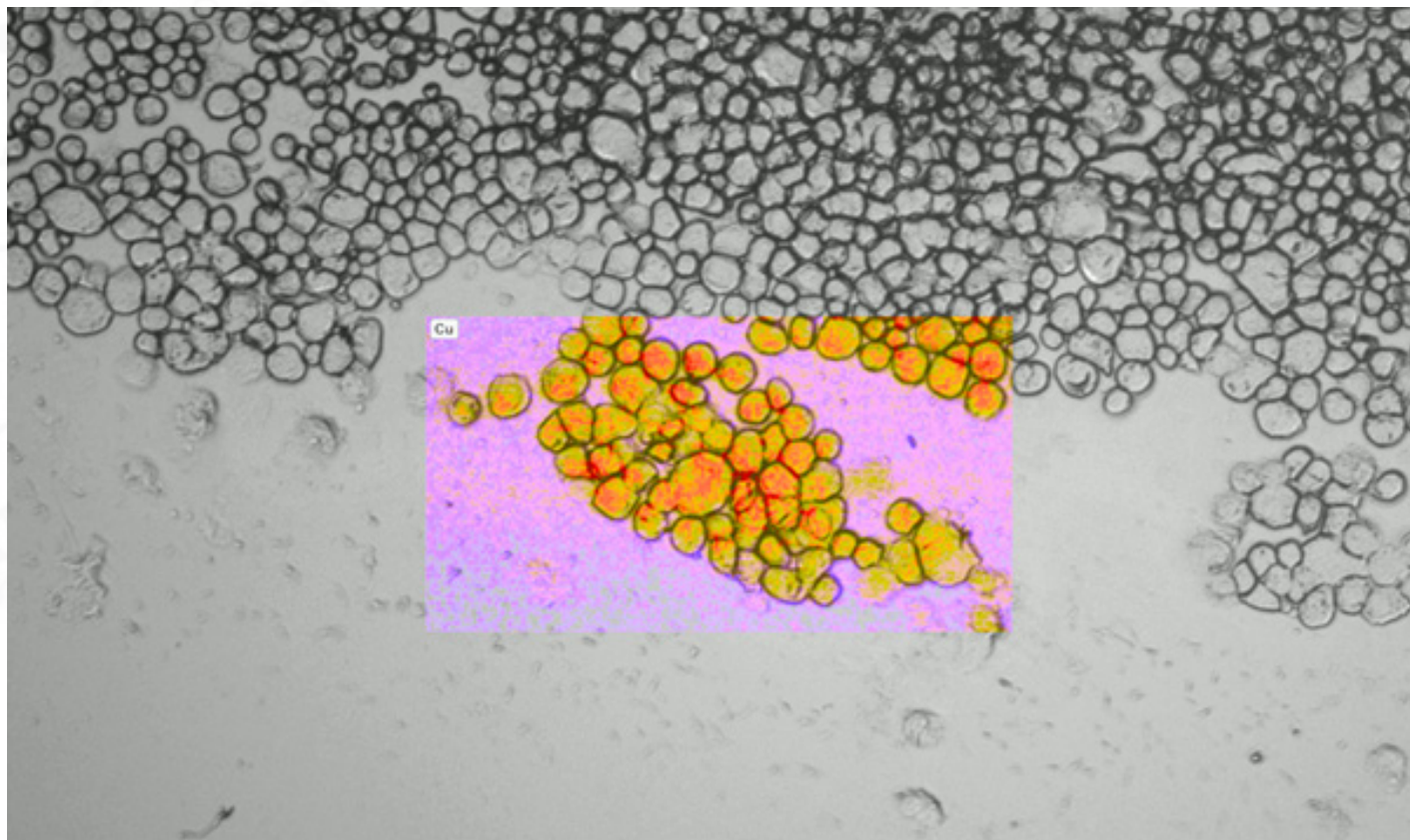
Figure 10. Cu distribution in single cells using a 1 μm spot, 100 Hz on imageBIO266. Courtesy of Dr Amy Managh, University of Loughborough.
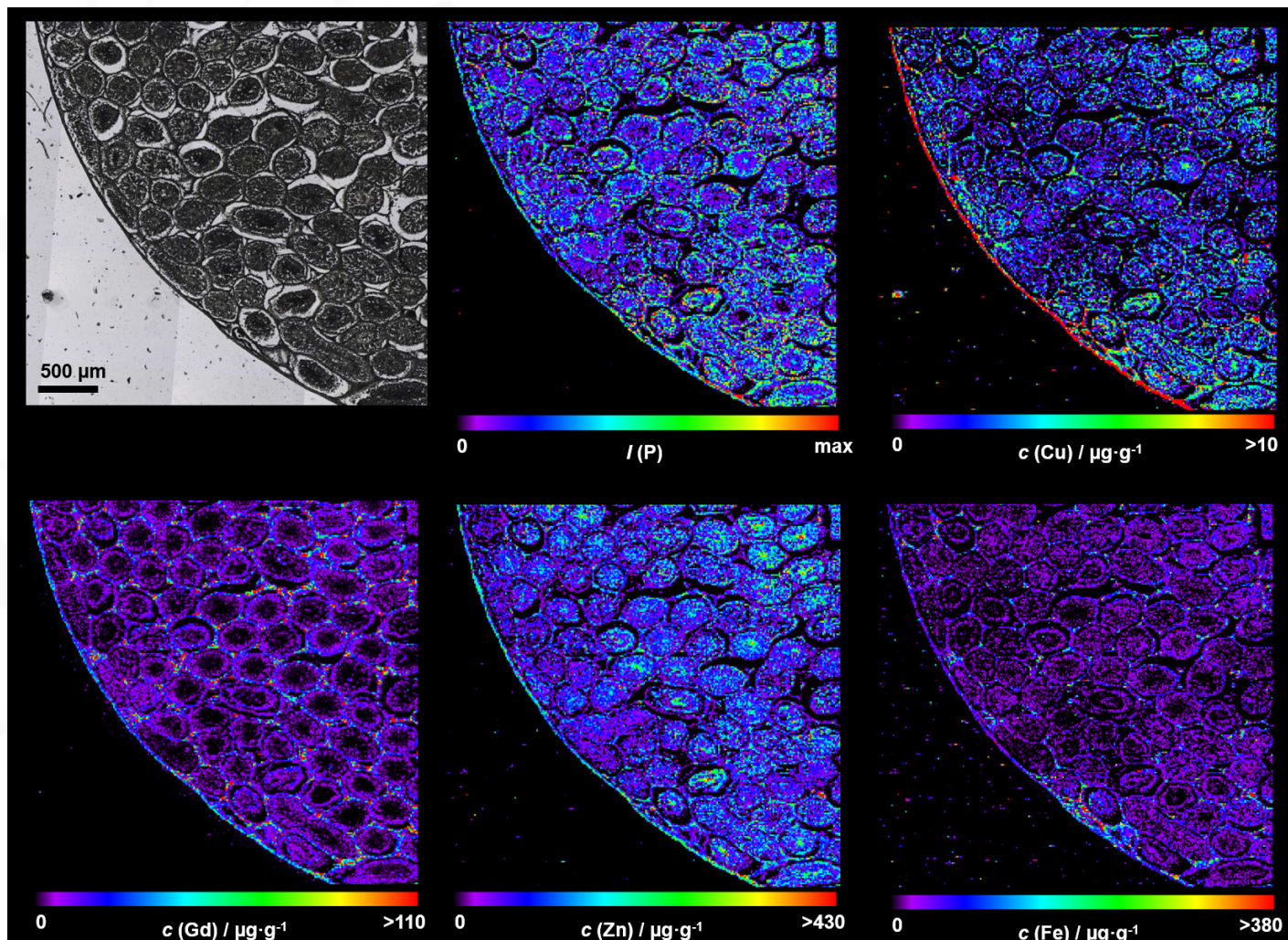
Figure 12. Multi-elemental imaging of rat testis to determine distribution of Gd following dosing with MRI contrast agent by LA-ICP-QMS using the imageBIO266.

Conclusions

The development studies and data from Elemental Scientific Lasers and our collaborators and users worldwide confirm the following conclusions:

- With the imageBIO266 the user sets parameters based on the sample itself and not the substrate underneath, and produces superior results in bioimaging experiments by LA-ICPMS.

- A 266 nm laser ablation system like the imageBIO266 provides the most highly-performing, versatile option for high speed bioimaging.

- The imageBIO266 is robust and space-efficient with cost of ownership at a fraction of an excimer laser.

- Experimental data shows that 266 nm outperforms 193 nm for bioimaging, offering a larger fluence bandgap between ablation of tissue and ablation of glass.

- Single-shot-total-consumption methods (LA-ICP-TOF-MS) at 266 nm are run at fluence levels below the threshold of ablation for glass, unlike 193 nm.

References

1. Thibaut Van Acker, et al. J. Anal. At. Spectrom., 2019, 34, 1957

2. Ingo Horn, Detlef Günther. Applied Surface Science 207 (2003) 144−157

3. M. Guillong, I. Horn and D. Günther. J. Anal. At. Spectrom., 2003, 18, 1224−1230.

4. S.M. Eggins, L.P.J. Kinsley, J.M.G. Shelley. Applied Surface Science 127−129 1998. 278−286

Elemental Scientific
L A S E R S